15TH IEA HEAT PUMP CONFERENCE
MAY 26–29, 2026 | HOFBURG
VIENNA 2026
DECARBONISATION THROUGH INNOVATION

Enhancing the compactness of propane heat pumps: a sensitivity analysis via dynamic modelling

Maged Dawoud[a,b*], Alice Mugnini[c], Alessia Arteconi[a,b]

[a]Department of Mechanical Engineering, KU Leuven, 3000 Leuven, Belgium
[b]EnergyVille, 3600 Genk, Belgium
[c]Dipartimento di Scienze Teoriche e Applicate, Università degli studi E-Campus, 22060 Novedrate, Italy

Abstract

The transition from conventional refrigerants, such as hydrofluorocarbons, to low-global-warming-potential alternatives, like natural hydrocarbons, is essential. Propane has been demonstrated to be a good option among the alternatives for residential heat pump systems despite its high flammability. To ensure safety when using flammable refrigerants, one practical approach is to reduce the refrigerant charge. Compact heat exchangers can facilitate this by minimizing the required refrigerant volume and maintaining reliable operation. However, this problem involves many interdependencies between the heat pump design and its operational behavior. Furthermore, over two-thirds of the refrigerant charge resides in the heat exchangers, highlighting their significant role in the system dynamics. In this context, this study investigates different heat pump sizing using a dynamic simulation model based on a moving-boundary approach. The work aims to analyse the refrigerant charge in an air-source heat pump across various operating conditions in order to provide indications for a more effective design. The results show the possibility to reduce the charge by one-third compared to typical design approaches based on manufacturer's specifications, while maintaining the outlet water temperature within ±1 K of the setpoint. These results demonstrate the need for more sophisticated tools to take into account the actual operating conditions in the design stage.

Selection and/or peer-review under the responsibility of the organizers of the 15th IEA Heat Pump Conference 2026.

Keywords: Heat Pump; Propane Charge; Dynamic Modelling; Moving Boundary; Compact Heat Exchangers.

1. Introduction

Traditional hydrofluorocarbons have been widely used as refrigerants in Heat Pumps (HPs); however, due to their environmental impacts, natural hydrocarbons are being utilized as sustainable alternatives [1]. These natural hydrocarbons offer favorable thermophysical properties and a low global warming potential. Among them, propane (R290) has been adopted as an alternative refrigerant for residential applications because it is highly energy efficient and entirely F-gas-free [2-3]. However, since propane is flammable, EU regulations, aligned with the IEC 60335-2-40 standard, limit its charge in residential HPs to less than 150 g for indoor installations [4]. Several studies have examined propane usage and its charge distribution across system components, the majority focuses on brine-to-water R290 HPs, a few address air-to-water R290 HP [5]. Most of these studies have been evaluated under the standard operating conditions (e.g., A0/W35 or B0/W35, i.e. air or brine at 0 ºC and sink water temperature at 35 ºC). Schnabel et al. [6] experimentally tested various configurations of propane BWHP, reporting a maximum Coefficient Of Performance (COP) of 4.5 at a specific charge of 24 g/kW under standard operating conditions. Sánchez-Moreno-Giner [7] investigated the experimental performance and refrigerant distribution of a 9.5 kW low-charge B0/W35 HP. At nominal conditions, almost 52% of the refrigerant was settled in the heat exchangers, with a specific charge of 20.5 g/kW and a reported COP of 3.2. On the other hand, Tang [8] tested an air-source propane HP and reported a maximum COP of 3.3 with a specific charge of 93.5 g/kW under A7/W35 operating conditions.

* Corresponding author. *E-mail address:* maged.dawoud@kuleuven.be

Given the wide range in specific charge and the limited literature on air-source HP, it is worth investigating further the impact of the design choices on the refrigerant charge. To design a highly efficient HP, mathematical optimization can be applied through detailed simulation models of the system. However, incorporating system dynamics into these models introduces complex interdependencies among the heat pump components (e.g., outdoor air temperature, compressor efficiency, and on-board control), making the resulting system-level model challenging to optimize. Several studies have shown the optimal design of an HP system with respect to the availability of energy source or component sizing, which significantly influence the overall investment costs [9-10]. Conventional heat pump sizing into an application is generally based on worst-case operating conditions, such as the peak heating load. However, this traditional approach becomes impractical when the peak load occurs for only a short period during the entire operating season. Therefore, this work aims to explore a range of heat pump sizes through a sensitivity analysis to identify the configurations that reduce refrigerant charge without compromising operational reliability. The analysis focuses on the refrigerant charge resulting from the change in internal volume and its effect on COP, thereby bridging design and operational aspects.

2. Methodology

To evaluate various heat pump sizing configurations, a model able to accurately assess the heat transfer inside the heat exchangers is required. A dynamic model of an air-source heat pump has been used for this purpose and is described in Section 2.1. Section 2.2 presents the case study considered in this work as a reference to illustrate the conventional sizing in design conditions. Subsequently, a sensitivity analysis is conducted to evaluate different configurations by varying the number of condenser plates and evaporator tubes, thereby assessing their impact on overall system performance. The methodology used for component sizing within the sensitivity analysis is summarized in Section 2.3.

2.1. Heat pump model

The air-source HP is modeled using a lumped-parameter dynamic model, which provides an accurate representation of the refrigerant flow and heat transfer in the system. The basic air-source HP consists of two heat exchangers, functioning as a condenser (COND) and an evaporator (EVAP), along with a compressor and a throttle valve. The dynamic model is developed using the moving-boundary approach that captures variations in heating demand while maintaining fast numerical convergence, making it suitable for iterative simulations and optimization studies. Moreover, the proposed dynamic model provides an efficient and robust framework for designing such energy systems, enabling both detailed performance evaluation and system design investigation.

2.1.1. Heat exchangers

Modelling low-charge HPs makes the governing dynamics concentrate in the heat exchangers, which hold more than two-thirds of the total refrigerant charge [11-12]. Therefore, the developed lumped model is characterized by time-varying phase boundaries within the heat exchangers. Model assumptions, which are typically adopted in the literature (e.g., [12-13]), are summarized in the following section, and more details can be found in [12-13].

Assumptions

- Both heat exchangers are considered one-dimensional in the flow direction.
- No work is done on or generated by the fluid.
- Gravitational forces and kinetic energy are neglected.
- Pressure drops across the heat exchangers are neglected (no axial variation), but temporal pressure changes are considered.
- Heat conduction and radiation are neglected.
- Viscous dissipation of refrigerant is neglected as it is too many orders of magnitude smaller than the energy between the refrigerant and the metal wall.
- Metal wall resistance is neglected.

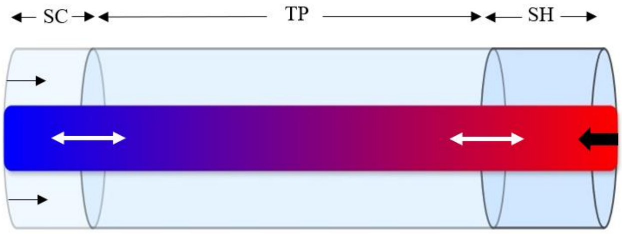

Figure 1: Schematic of the moving boundary model for both heat exchangers, black arrows indicate the flow of propane (bold) and the secondary fluid (normal), while white arrows represent the time-varying phase boundaries between zones (SH-TP-SC).

Applying these assumptions to the general conservation equations of mass, momentum, and energy eliminates the need for the momentum equation. To derive the governing equations, the refrigerant mass balance, Eq. (1), refrigerant energy balance, Eq. (2), metal wall energy balance, Eq. (3), and secondary fluid energy balance, Eq. (4), are integrated according to Leibniz's rule [13]. The COND has been divided into three zones based on phase: superheating (SH), two-phase (TP), and subcooling (SC), as shown in Figure 1. In contrast, the EVAP has been divided into two zones: TP and SH. As a result, the number of equations to be solved depends on the number of zones/phase regions that exist in each heat exchanger. The COND type is a plate heat exchanger, whereas the EVAP is a finned tube heat exchanger, with their respective geometrical parameters provided in Section 2.2.

$$\frac{\partial \rho_r}{\partial t} + \frac{\partial (\rho v)_r}{\partial L} = 0 \tag{1}$$

$$\frac{\partial (\rho u)_r}{\partial t} + \frac{\partial (\rho u v + p v)_r}{\partial L} + \frac{\partial (\alpha\, \Delta T)_r}{\partial L} = 0 \tag{2}$$

$$\left(c_p \rho A\right)_m \frac{\partial T_m}{\partial t} - \frac{\partial (\alpha\, \Delta T)_r}{\partial L} + \frac{\partial (\alpha\, \Delta T)_{sf}}{\partial L} = 0 \tag{3}$$

$$\left(c_p \rho A\right)_{sf} \frac{\partial T_{sf}}{\partial t} - \left(c_p \rho A v\right)_{sf} \frac{\partial T_{sf}}{\partial L} - \frac{\partial (\alpha\, \Delta T)_{sf}}{\partial L} = 0 \tag{4}$$

The mass and energy balances are represented in equations (1-4), where the subscript r refers to the refrigerant, m to the metal wall, and sf denotes the secondary fluid, either water or air. ρ is density, t is time, v is velocity, L is the length in the flow direction, u is internal energy, p is pressure, A is the cross-sectional area, c_p is the specific heat capacity, and ΔT is the temperature difference between the refrigerant or the secondary fluid and the metal wall. The heat transfer coefficient, α, is determined using the references in Table 1, with experimental correlations that depend on the refrigerant phase/secondary fluid type, as well as the heat exchanger type.

Table 1: Correlations used for heat transfer coefficient calculations in the heat exchangers.

Phase	Condenser	Evaporator
SH	[14]	[15]
TP	[16]	[17]
SC	[18-19]	-
Water/air	[18-19]	[20]

2.1.2. Compressor

A variable-speed scroll compressor is used, featuring propane as the working fluid. The compressor is selected based on the technical data provided by Copeland for propane YHV models [21]. Furthermore, it was experimentally investigated by Ossorio et al. in their study [22]. Eq. (5) calculates the compressor mass flow rate $\dot{m}_{CM}$, where V_h is the stroke volume, Z_{CM} is the compressor frequency, ρ_{suc} is the refrigerant density at the suction point and η_v is the volumetric efficiency.

$$\dot{m}_{CM} = V_h\, Z_{CM}\, \rho_{suc}\, \eta_v \tag{5}$$

The discharge enthalpy h_{dis} is also calculated using Eq. (6) as a function of the specific isentropic work $(h_{dis,s} - h_{suc})$, suction enthalpy h_{suc}, and isentropic efficiency η_s. Both η_v and η_s are determined based on the empirical correlations proposed by Guth [23].

$$h_{dis} = \frac{h_{dis,s} - h_{suc}}{\eta_s} + h_{suc} \tag{6}$$

2.1.3. Throttle valve

The throttle valve is chosen based on a maximum heating capacity of 12 kW using Danfoss Coolselector®2 online software for electronic expansion valves [24]. The mass flow rate of the throttle valve is calculated using Eq. (7) as proposed by both Liu and Ma [25-26].

$$\dot{m}_{TV} = C_D\, A_{open} \sqrt{2\, \rho_i\, |p_i - p_o|} \tag{7}$$

Where C_D is the discharge coefficient calculated using the work of Li, i & o are subscripts for the inlet & the outlet of the valve, respectively, and A_{open} is the valve opening area [27].

2.1.4. Propane charge

The propane charge for each design configuration is determined by the internal volumes of the four main components of the HP and the interconnecting lines. While the compressor and expansion valve volumes remain constant across all design configurations, the COND and EVAP volumes vary with the selected geometry. For each heat exchanger, the charge is obtained by multiplying the volume of each zone by its corresponding refrigerant density, as illustrated in Figure 1. Additionally, all thermophysical properties of propane, including density, have been calculated according to the work of Dawoud et al. [28], which is based on fast regression models validated against CoolProp [29] and applied in dynamic modelling. The developed HP model adjusts the compressor speed and valve opening to compute their respective mass flow rates (equations (5) and (7)), and convergence is achieved only when these two rates satisfy the whole system mass balance. The model is implemented and solved using the GEKKO library in Python [30], employing a convergence criterion in which the error between two consecutive iterations is set to less than 10^{-5}.

2.2. Case study

A residential installation in Belgium is selected as the case study to perform the analysis. According to the Royal Meteorological Institute [31], the typical winter period in Belgium extends from December 1 to the end of February. The duration curve of the Belgian winter outdoor air temperatures is shown in Figure 2. Considering a typical Belgian house (which is a two-floor detached single-family house with a net floor area of 194 m²), a representative heating demand duration curve is obtained (Figure 2, see reference [32] for further details).

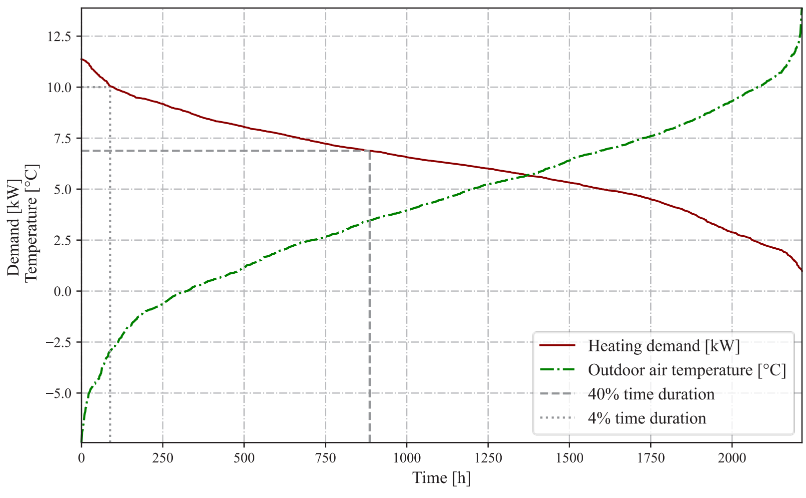

Figure 2: Heating demand duration curve and outdoor air temperature for Belgium during the winter season (Uccle, Belgium).

Based on the outdoor air temperature data, the minimum temperature recorded is –7.4 °C. Under these conditions, the heating demand reaches a peak of 11.4 kW, with only 4% of the time exceeding 10 kW, and 7 kW meets the demand for over 60% of the total operating time.

Using a conventional approach (peak load: 12 kW, source temperature: –8 °C) and based on manufacturer specifications, it was possible to size the heat pump heat exchangers: the condenser is a brazed plate heat exchanger composed of 22 plates (provided by Alfa Laval [33]), while the evaporator is a finned tube heat exchanger with estimated 120 tubes to satisfy the peak load [15] (values consistent with the findings of Reichl's work [34]). All remaining geometric parameters are summarized in Table 2. This conventional design has been selected to represent a heat pump intended to operate continuously in an efficiency-oriented mode, without the use of auxiliary or backup heaters. As such, the unit must be capable of meeting the full heating demand under worst-case operating conditions, which remains a common sizing criterion for commercially available market products.

Table 2: Geometric parameters of the condenser and evaporator used in the dynamic model

Parameter	Value	Unit
Condenser		
Number of plates	10-22	-
Plate length	324	mm
Plate width	95	mm
Plate thickness	0.2	mm
Corrugation angle	55	º
Height of corrugation	1.5	mm
Material of plates	SS 316	-
Evaporator		
Number of rows	4-8	-
Number of tubes/row	10/12/15	-
Tube length	650	mm
Tube inside diameter	5	mm
Tube/fin thickness	0.6/0.25	mm
Fin spacing	2	mm
Longitudinal/Transversal tube pitch	22/20	mm
Material of tubes/fins	Cu/Al	-

2.3. Sensitivity analysis

A sensitivity analysis is performed to evaluate the HP performance across several HP configurations obtained by varying the heat exchangers size, considering a 50% reduction in internal volume. The assumptions for the analysis are summarized as follows:

- An energy source temperature of –8 °C was selected, consistent with the minimum outdoor temperature of –7.4 °C.
- The outlet water temperature was set to 40 °C with a temperature difference (ΔT) of 10 °C, in accordance with standards [35-36].
- The number of condenser plates evaluated ranged from 10 to 22, with 22 representing the conventional heat pump design provided by Alfa Laval [15-33] (see Section 2.2).
- Evaporator rows were analyzed from 4 to 8, with three tube configurations per row (10, 12, and 15), where the upper limit, 8, was determined based on LMTD calculations [15].
- The compressor is a YHV variable-speed scroll model and has a swept volume of 46 cm^3 with an operating frequency range of 15–120 Hz, selected based on the technical data provided by Copeland [21].
- The throttle valve type is ETS 5M20 with an orifice size of 2 mm, and selected with the help of Danfoss Coolselector®2 online software for electronic expansion valves [24].
- The lengths of the interconnecting lines follow the values reported by Li et al. [37]: the vapor lines are maintained as specified (1.2 m discharge line and 5.8 m suction line), whereas the liquid line is shortened to 0.3 m to minimize the refrigerant charge associated with the liquid phase.

- Three heating demand levels (7, 10, and 12 kW) are selected to evaluate the system behavior across a range of operating conditions. While the 12 kW represents the peak load, the additional levels of 10 kW and 7 kW are included to investigate performance under more typical loads corresponding to the 96% and 60% time-exceedance levels, respectively.
- The model of each HP configuration is run for the three heating demand levels (7, 10, 12 kW) and it calculates the charge of the system (according to section 2.1.4) that satisfies all these representative working conditions.

3. Results and Discussion

First, an overview of the model's dynamic behavior under the three heating demand levels is presented in Section 3.1. Afterwards, all design configuration combinations are evaluated using the dynamic model under the same operating conditions. An overall summary of the results is presented in Section 3.2, with a detailed discussion of the allowable maximum power.

3.1. HP dynamics

The dynamic behavior of the HP model is illustrated in Figure 3, which shows the zone lengths of both heat exchangers for three different heating demand levels. While the TP zone dominates most of the COND volume with almost 60% of the plate length, the EVAP TP length increases progressively with increasing heat demand from 7 to 12 kW. In contrast, the evaporator SH length decreased from approximately 65% to 40%. This change keeps the superheating constant at 7 K for the different demand levels. The COND zone lengths (SH-TP-SC) show slight variation across different heating demands, as the water setpoint temperature is fixed at 40 °C for all cases.

Understanding the transient evolution of the zone lengths in the heat exchangers is essential because the refrigerant distribution (i.e., its density), and consequently the total charge, is strongly dependent on the dynamic behavior of the system. By capturing how the SH or TP regions evolve under varying heating demand levels, the model reveals operational constraints that are not observable with steady-state approaches (e.g., SH instability or minimum TP length during transients). This insight is crucial for designing more compact heat exchangers while reliably meeting performance requirements.

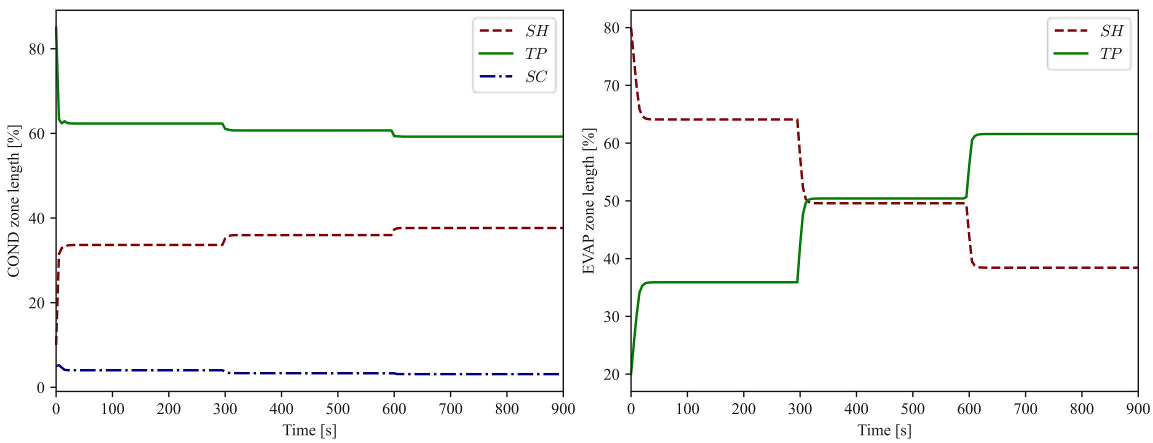

Figure 3: Dynamic time-varying zone lengths of the condenser (left) and the evaporator (right) for the design configuration (COND16 & EVAP4x12).

3.2. Sensitivity analysis

Several design configurations have been evaluated using the dynamic model, with the case of 22 COND plates and 8x15 EVAP tubes serving as the reference case, as specified in Section 2.2. The charge-reduction calculations values in Figure 4 are calculated relative to this reference case. Based on the change in the number of COND plates and EVAP tubes, the refrigerant charge differs across the various design configurations, as explained in Section 2.1.4. Varying the COND plates while keeping the number of EVAP tubes constant leads to a maximum charge reduction of 33.7% (vertical difference in Figure 4). On the other hand, changing the EVAP tubes while holding the number of COND plates constant results in a much smaller maximum reduction of only 13.2% (horizontal difference in Figure 4). This highlights that the COND is generally more impactful in air-source HPs, as a large portion of the refrigerant charge accumulates there due to the high refrigerant density of the subcooled region.

The power shown in Figure 4 represents the maximum allowable power achievable at each design configuration. This work aims to introduce the guidelines of a more effective design approach, which does not depend on the peak load (12 kW) but instead on the time duration of each load in favor of the charge. For instance, by analyzing the heating demand duration curve for Belgium during the winter season (Figure 2), it is found that loads above 10 kW occur for only 4% of the time during the winter season. Therefore, the design aspect based on the peak load is no longer a favorable option for heat pumps using flammable refrigerants such as propane.

In this study, the conventional HP design configuration (COND22 and EVAP8×15) is first presented in Section 2.2, with a specific charge of 8 g/kW at operating conditions (A-8/W40). As shown in Figure 4, several 18-plate configurations can still deliver 12 kW with a reduced refrigerant charge of up to 20%, indicating that typical manufacturer sizing overestimates the required heat-exchanger volume and that achieving peak demand does not necessarily require larger units but rather more compact heat exchangers. Additionally, all design configurations with 14 or more COND plates can achieve a heating load of 10 kW or higher. But by limiting the design load to 10 kW, it becomes possible to achieve more than a 20% reduction in refrigerant charge with only 14 COND plates across the different EVAP tube configurations.

Building on this assessment, the preliminary guidelines for an alternative design methodology are evaluated in this section. The proposed approach examines the feasibility of sizing the heat pump based on reduced peak-load conditions but at the same operating conditions, with the aim of enhancing safety and optimizing refrigerant use. Therefore, although the design configurations with 18 COND plates satisfy the peak load of 12 kW, this study recommends using a lower-demand option (e.g., COND14 and EVAP4x15), with a charge reduction of almost 31% and a specific charge of 6.7 g/kW under operating conditions (A-8/W40). This concludes that around one-third of the charge could be saved by reducing the design capacity by just 2 kW. Backup heaters offer a straightforward alternative to cover the difference to peak load (only 4% of the total operating time); however, the choice involves a trade-off between refrigerant charge and COP.

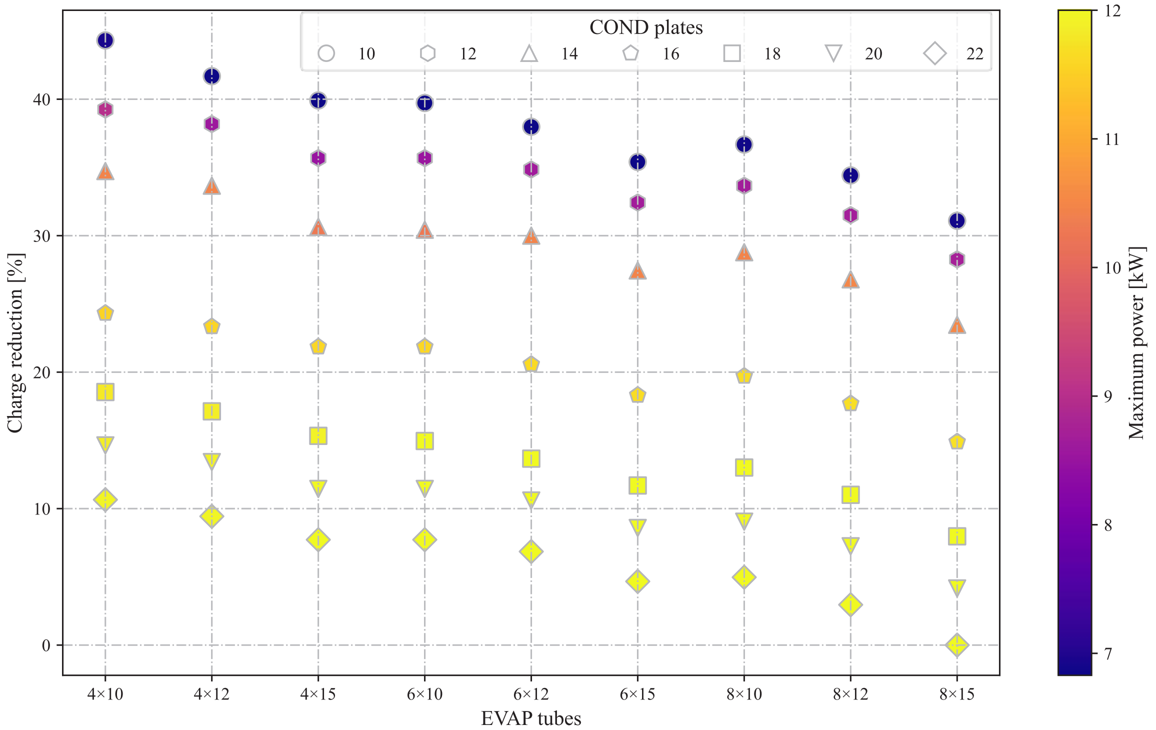

Figure 4: Sensitivity analysis results quantifying charge reduction and the maximum allowable power (encoded in the color bar) across the different design configurations.

To better analyze the various design configurations, both the COP and the outlet water temperature are shown in Figure 5. While the outdoor air temperature was held constant at -8 °C, the outlet water temperature remained consistent within ±1 K of the setpoint, as shown in Figure 5 (right). The COP varies between 2.75 and 3.1 under the operating conditions A-8/W40. This variation is explained by two main factors: the minor deviation in outlet water temperature (only ±0.3% of the setpoint) and the heat transfer area on the source side (EVAP tubes). The second effect is particularly evident in cases where the outlet temperature is nearly constant, yet the COP still shows slight variations (e.g., for 10, 18, 20, and 22 COND plates). Overall, these results indicate that COP is influenced not only by the COND design, which affects the outlet water temperature, but also by the EVAP design, even when the source temperature remains constant.

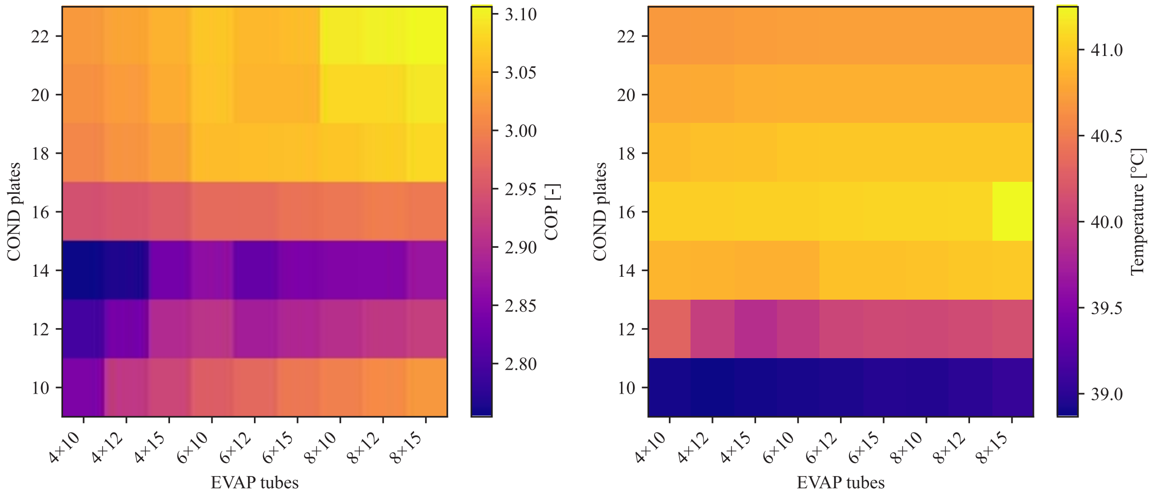

Figure 5: Sensitivity analysis coefficient of performance (left) and outlet water temperature (right).

4. Conclusion

Compact heat exchangers are a key technology for meeting safety requirements when using flammable refrigerants such as propane. Consequently, evaluating different HP design approaches is highly valuable. Over 60 design configurations have been tested to assess their maximum achievable power and the potential for reducing refrigerant charge while maintaining acceptable performance. The conventional HP design based solely on peak load is not ideal for systems using flammable refrigerants. To address this, basic guidelines for a new design approach have been proposed, showing the potential of sizing the HP on reduced peak loads. The results show the possibility of reducing the refrigerant charge by more than 31% compared to the typical design condition and manufacturer's specification, while keeping the outlet water temperature within 0.8 K of the setpoint and a COP of 2.8 at the operating conditions (A-8/W40). These results demonstrate that new design approaches focused on minimizing refrigerant charge are essential for HPs operating with flammable refrigerants. Furthermore, future integration of global optimization frameworks with dynamic modelling can lead to HP designs that effectively balance system compactness and operational performance.

Acknowledgements

This research has been financially supported by KU Leuven through the C2 project No. 3E230127.

References

[1] L. Liansheng, "Research Progress on Alternative Refrigerants and Their Development Trend," *Journal of Refrigeration Magazines Agency Co., Ltd.*, vol. 32, pp. 53–58, 2011.

[2] European Commission, "The availability of refrigerants for new split air conditioning systems that can replace fluorinated greenhouse gases or result in a lower climate impact," Brussels, Sep. 2020. Accessed: Oct. 12, 2025. [Online]. Available: https://climate.ec.europa.eu/system/files/2020-

09/c_2020_6637_en.pdf
[3] C. Höges *et al.*, “Low-GWP refrigerants in heat pumps: An experimental investigation of the influence of an internal heat exchanger,” *Energy Conversion and Management: X*, vol. 24, p. 100704, Oct. 2024, doi: 10.1016/j.ecmx.2024.100704.
[4] IEC 60335-2-40, *Household and similar electrical appliances - safety - Part 2-40: Particular requirements for electrical heat pumps, air-conditioners and dehumidifiers*. International Electrotechnical Commission, 2022.
[5] A. A. Bani Issa, C. Liang, E. A. Groll, and D. Ziviani, “Residential heat pump and air conditioning systems with propane (R290) refrigerant: Technology review and future perspectives,” *Appl. Therm. Eng.*, vol. 266, p. 125560, May 2025, doi: 10.1016/J.APPLTHERMALENG.2025.125560.
[6] L. Schnabel, T. Methler, A. H. Hassan, C. Dankwerth, and J. M. G. Maciá, “Design and Analysis of Charge-Reduced Refrigerant Cycles Using R290,” *Chemie Ingenieur Technik*, vol. 95, no. 3, pp. 353–362, Mar. 2023, doi: 10.1002/cite.202200150.
[7] L. Sánchez-Moreno-Giner, T. Methler, F. Barceló-Ruescas, and J. Gonzálvez-Maciá, “Refrigerant charge distribution in brine-to-water heat pump using R290 as refrigerant,” *International Journal of Refrigeration*, vol. 145, pp. 158–167, Jan. 2023, doi: 10.1016/J.IJREFRIG.2022.10.013.
[8] W. Tang, G. He, S. Zhou, W. Sun, D. Cai, and K. Mei, “The performance and risk assessment of R290 in a 13 kW air source heat pump,” *Appl. Therm. Eng.*, vol. 144, pp. 392–402, Nov. 2018, doi: 10.1016/J.APPLTHERMALENG.2018.08.070.
[9] G. Bagarella, R. Lazzarin, and M. Noro, “Sizing strategy of on–off and modulating heat pump systems based on annual energy analysis,” *International Journal of Refrigeration*, vol. 65, pp. 183–193, May 2016, doi: 10.1016/J.IJREFRIG.2016.02.015.
[10] T. Beck, H. Kondziella, G. Huard, and T. Bruckner, “Optimal operation, configuration and sizing of generation and storage technologies for residential heat pump systems in the spotlight of self-consumption of photovoltaic electricity,” *Appl. Energy*, vol. 188, pp. 604–619, Feb. 2017, doi: 10.1016/J.APENERGY.2016.12.041.
[11] M. Dawoud and A. Arteconi, “Novel Design Approach for Propane Heat Pump Using Dynamic Modelling,” in *Book of Abstracts of the 11th Heat Powered Cycles Conference*, 2025, pp. 85–88. Accessed: Nov. 15, 2025. [Online]. Available: https://lirias.kuleuven.be/4270243&lang=en
[12] A. Desideri *et al.*, “Comparison of moving boundary and finite-volume heat exchanger models in the Modelica language,” *Energies (Basel).*, vol. 9, no. 5, 2016, doi: 10.3390/en9050339.
[13] S. Bendapudi, J. E. Braun, and E. A. Groll, “A comparison of moving-boundary and finite-volume formulations for transients in centrifugal chillers,” *International Journal of Refrigeration*, vol. 31, no. 8, pp. 1437–1452, Dec. 2008, doi: 10.1016/J.IJREFRIG.2008.03.006.
[14] G. A. Longo, “The effect of vapour super-heating on hydrocarbon refrigerant condensation inside a brazed plate heat exchanger,” *Exp. Therm. Fluid Sci.*, vol. 35, no. 6, pp. 978–985, Sep. 2011, doi: 10.1016/J.EXPTHERMFLUSCI.2011.01.018.
[15] M. J. . Moran, H. N. . Shapiro, D. D. . Boettner, and M. B. . Bailey, *Fundamentals of Engineering Thermodynamics*, 7th ed. Wiley, 2011.
[16] G. A. Longo, G. Righetti, and C. Zilio, “A new computational procedure for refrigerant condensation inside herringbone-type Brazed Plate Heat Exchangers,” *Int. J. Heat Mass Transf.*, vol. 82, pp. 530–536, Mar. 2015, doi: 10.1016/J.IJHEATMASSTRANSFER.2014.11.032.
[17] M. A. H. Ghazali, Y. Mohd-Yunos, A. S. Pamitran, O. Jong-Taek, and N. Mohd-Ghazali, “Development of a new correlation for pre-dry out evaporative heat transfer coefficient of R290 in a microchannel,” *International Journal of Air-Conditioning and Refrigeration*, vol. 30, no. 1, p. 15, 2022, doi: 10.1007/s44189-022-00015-3.
[18] M. B. Kim and C. Y. Park, “An experimental study on single phase convection heat transfer and pressure drop in two brazed plate heat exchangers with different chevron shapes and hydraulic diameters,” *Journal of Mechanical Science and Technology*, vol. 31, no. 5, pp. 2559–2571, 2017, doi: 10.1007/s12206-017-0454-0.
[19] A. S. Wanniarachchi, U. V. Ratnam, B. E. Tilton, and K. Dutta-Roy, “Approximate correlations for chevron-type plate heat exchangers,” 1995. [Online]. Available: https://api.semanticscholar.org/CorpusID:113298711
[20] H. Kalantari, S. A. Ghoreishi-Madiseh, J. C. Kurnia, and A. P. Sasmito, “An analytical correlation for conjugate heat transfer in fin and tube heat exchangers,” *International Journal of Thermal Sciences*, vol. 164, p. 106915, Jun. 2021, doi: 10.1016/J.IJTHERMALSCI.2021.106915.
[21] Copeland, “Scroll Variable Speed Compressors,” Copeland.com. Accessed: Oct. 03, 2025. [Online]. Available: https://www.copeland.com/en-gb/shop/copeland-scroll-yhv1u-compressors
[22] R. Ossorio and E. Navarro-Peris, “Study of oil circulation rate in variable speed scroll compressor working with propane,” *International Journal of Refrigeration*, vol. 123, pp. 63–71, Mar. 2021, doi:

10.1016/J.IJREFRIG.2020.12.002.

[23] T. Guth and B. Atakan, "Semi-empirical model of a variable speed scroll compressor for R-290 with the focus on compressor efficiencies and transferability," *International Journal of Refrigeration*, vol. 146, pp. 483–499, Feb. 2023, doi: 10.1016/J.IJREFRIG.2022.10.024.

[24] Danfoss, "Coolselector®2," Danfoss.com. Accessed: Oct. 03, 2025. [Online]. Available: https://www.danfoss.com/en/service-and-support/downloads/dcs/coolselector-2/#tab-overview

[25] H. Liu, J. Cai, and D. Kim, "A hierarchical gray-box dynamic modeling methodology for direct-expansion cooling systems to support control stability analysis," *International Journal of Refrigeration*, vol. 133, pp. 191–200, Jan. 2022, doi: 10.1016/J.IJREFRIG.2021.10.013.

[26] J. Ma, D. Kim, J. E. Braun, and W. T. Horton, "Development and validation of a dynamic modeling framework for air-source heat pumps under cycling of frosting and reverse-cycle defrosting," *Energy*, vol. 272, p. 127030, Jun. 2023, doi: 10.1016/J.ENERGY.2023.127030.

[27] W. Li, "Simplified modeling analysis of mass flow characteristics in electronic expansion valve," *Appl. Therm. Eng.*, vol. 53, no. 1, pp. 8–12, Apr. 2013, doi: 10.1016/J.APPLTHERMALENG.2012.12.035.

[28] M. Dawoud, A. Mugnini, and A. Arteconi, "Fast Explicit Formulations of Propane Thermophysical Properties for Dynamic Modelling," *Energies (Basel).*, vol. 19, no. 4, p. 892, Feb. 2026, doi: 10.3390/en19040892.

[29] I. H. Bell, J. Wronski, S. Quoilin, and V. Lemort, "Pure and pseudo-pure fluid thermophysical property evaluation and the open-source thermophysical property library coolprop," *Ind. Eng. Chem. Res.*, vol. 53, no. 6, pp. 2498–2508, Feb. 2014, doi: 10.1021/ie4033999.

[30] L. D. R. Beal, D. C. Hill, R. A. Martin, and J. D. Hedengren, "GEKKO Optimization Suite," *Processes*, vol. 6, no. 8, p. 106, Jul. 2018, doi: 10.3390/pr6080106.

[31] KMI, "Klimaatstatistieken van de Belgische gemeenten," RMI/KMI. Accessed: Oct. 08, 2025. [Online]. Available: https://www.meteo.be/en/belgium

[32] M. Evens and A. Arteconi, "Representative cycle for heat pump energy flexibility evaluations – A comparative simulation study of existing day selection procedures to a new consecutive day procedure," *Energy Build.*, vol. 297, p. 113443, Oct. 2023, doi: 10.1016/J.ENBUILD.2023.113443.

[33] Alfa Laval, "Brazed Plate Heat Exchangers." Accessed: Nov. 10, 2025. [Online]. Available: https://www.alfalaval.com/

[34] C. Reichl, C. Sandström, F. Hochwallner, F. Linhardt, M. Popovac, and J. Emhofer, "Frosting in heat pump evaporators part A: Experimental investigation," *Appl. Therm. Eng.*, vol. 199, p. 117487, Nov. 2021, doi: 10.1016/J.APPLTHERMALENG.2021.117487.

[35] EN 14511-2, *Tracked Changes. Air conditioners, liquid chilling packages and heat pumps for space heating and cooling and process chillers, with electrically driven compressors. Part 2, Test conditions*. British Standards Institution, 2022.

[36] EN 14825, *Air conditioners, liquid chilling packages and heat pumps, with electrically driven compressors, for space heating and cooling, commercial and process cooling. Testing and rating at part load conditions and calculation of seasonal performance*. British Standards Institution, 2022.

[37] T. Li *et al.*, "Measurement of refrigerant mass distribution within a R290 split air conditioner," *International Journal of Refrigeration*, vol. 57, pp. 163–172, Sep. 2015, doi: 10.1016/J.IJREFRIG.2015.05.012.